

Application of the Global Positioning System to the Measurement of Overhead Power Transmission Conductor Sag

Chris Mensah-Bonsu, *Member, IEEE*, Ubaldo Fernández Krekeler, *Student Member, IEEE*, Gerald Thomas Heydt, *Fellow, IEEE*, Yuri Hoverson, John Schilleci, *Senior Member, IEEE*, and Baj L. Agrawal, *Fellow, IEEE*

Abstract—This paper describes a method to directly measure the physical sag of overhead electric power transmission conductors. The method used relies on the global positioning system (GPS) used in the differential mode. The direct measurement of sag is a main advantage of the concept. The digital signal processing required is described in detail in a four-level configuration. Typical accuracy, response time, problems, strengths, and weaknesses of the method are also described.

Index Terms—Conductor clearance warning, conductor sag, dynamic thermal line rating, global positioning system (GPS), Open Access Same Time Information System (OASIS), overhead conductors, transmission engineering.

I. OVERHEAD CONDUCTOR RATINGS

UNDER deregulation of the power industry in the United States, electric utilities are under pressure to make optimum use of their existing facilities, of which the overhead transmission system is usually a principal component. Overhead conductors form the backbone of power transmission systems. The ratings of circuits are critical to system capability. Real time conductor rating holds promise for the maximization of system transfer capability.

The transmission capacity of overhead conductors depends on the ambient temperature, wind speed, wind direction, incident solar radiation, limiting physical conductor characteristics, and conductor configuration/geometry. The conductor loading capacity is computed *statically* or *dynamically*. In the static case, a worst-case weather condition is assumed while in the dynamic case, the actual weather condition is taken into account. In either case, the conductor load must produce a conductor temperature so that there is no loss of strength by annealing or creep. One must operate the circuit so that the mandated clearances are not violated.

Experience in some utilities shows that the clearance of an overhead conductor is a key factor limiting its thermal capacity,

especially in regions of high interconnection. An ultimate measure of the conductor rating is the physical sag of the conductor, and the continuous monitoring of the conductor clearance may improve system operation. This paper considers the use of a GPS-based measurement system for overhead conductor sag based on tests using a laboratory breadboarded prototype.

Traditionally, conductor sag has been considered by indirect measurements. Recently, commercialized techniques include the physical measurement of conductor surface temperature using an instrument mounted directly on the line and a second instrument that measures conductor tension at the insulator supports. These measured parameters can be used to estimate conductor sag. The pertinence of conductor sag to circuit operation relates to the calculation of a *dynamic thermal* rating of the line, considering the ambient conditions and present operating regime [1]–[5]. Measuring conductor sag is not equivalent to rating lines, but in this paper a novel sag measurement technique is offered as an aid to transmission line rating. Real-time measurement of overhead conductor sag can be used for conductor clearance warning purposes to ensure that mandated clearance limits are not violated. Furthermore, real-time conductor sag information has the potential of being accurately converted to dynamic line ratings. These dynamic line ratings may then be useable in connection with system studies to determine the maximum transmission capacity of circuits. In a deregulated electric utility environment, transmission circuit ratings assume renewed importance because some companies are marketing transmission access. A widely used system for transmission capacity sales is known as the Open Access Same Time Information System (OASIS). To be able to rapidly and accurately determine the dynamic transmission line rating of a circuit has obvious pecuniary value in OASIS. It is worth mentioning that dynamic thermal line rating is beyond the scope of this paper.

II. GLOBAL POSITIONING SYSTEM

Based on a constellation of 24 satellites, the Navigation Satellite Timing and Ranging (NAVSTAR) GPS was developed, launched, and maintained by the United States government as a worldwide navigation and positioning resource for both military (i.e., precise positioning service) and civilian (i.e., standard positioning service) applications. The method relies

Manuscript received September 1, 1999; revised May 5, 2001.

C. Mensah-Bonsu is with the California Independent System Operator, Folsom, CA 95630 USA.

U. Fernández Krekeler is with the Paraguayan Electricity Authority, Asunción, Paraguay.

G. T. Heydt and Y. Hoverson are with Arizona State University, Tempe, AZ 85287 USA.

J. Schilleci is with Entergy, New Orleans, LA 70112 USA.

B. L. Agrawal is with Arizona Public Service, Phoenix, AZ 85001 USA.

Publisher Item Identifier S 0885-8977(02)00576-9.

on accurate time-pulsed radio signals in the order of nanoseconds from high altitude Earth orbiting satellites of about 11 000 nautical miles, with the satellites acting as precise reference points. These signals are transmitted on two carrier frequencies known as the L1 and L2 frequencies. The L1 carrier is 1.5754 GHz and carries a pseudo-random code (PRC) and the status message of the satellites. There exist two pseudorandom codes: the coarse acquisition (C/A) and the precise (P) codes. The L2 carrier is 1.2276 GHz and is used for the more precise military PRC. The signals from four or more satellites are received by a specially designed GPS receiver, and the following simultaneous equations are solved

$$(X_{sk} - X_{rj})^2 + (Y_{sk} - Y_{rj})^2 + (Z_{sk} - Z_{rj})^2 = (R_k - dT)^2$$

$$k = 1, 2, \dots, n \quad n \geq 4 \quad (1)$$

where (X_{sk}, Y_{sk}, Z_{sk}) represents the k th satellite position (X_{rj}, Y_{rj}, Z_{rj}) denotes the unknown j th receiver position, R_k denotes the range to the k th satellite, and dT is the unknown receiver clock bias converted to distance. This gives the longitude and latitude of the receiver (i.e., effectively x and y), the altitude of the receiver (effectively z), and the time that the measurement was made t . Interestingly, the GPS transmission is made at low power level (the signal strength at the point of reception is about -90 to -120 dBm). At this power level, the SNR is very low at the surface of the Earth. The attenuation of the noise is accomplished by averaging the received signal. The noise is averaged and a distinctively coded signal appears as an output. The averaging process, as well as the solution of (1) are the main time limiting processes that determine how often a GPS measurement can be made.

Perhaps the most often asked question about GPS technology relates to its accuracy. The ultimate accuracy of position measurements made using the GPS depend on a variety of factors (e.g., the type of measurement made, x , y , or z , ionospheric and tropospheric conditions, government inserted error effected as a security measure, number of satellites in view, receiver equipment used, digital signal processing of the received signal, surface features, reflection of signals, and other factors). Table I summarizes some of these interacting factors and the approximate error.

In Table I, a differential mode of measurement is also shown, and this is discussed later. The greatest source of error is the intentional insertion of error through a subsystem known as selective availability (SA). This error is inserted by the government as a security measure. Authorized noncivilian users of a special high accuracy mode of operation have a special mechanism to decode the SA and eliminate the intentional error.

The differential GPS (DGPS) mode is generally used in order to decrease the SA error. This mode consists of the use of two GPS receivers, the *base*, and the *rover*. The actual position of the base is known (e.g., by precise surveying) and compared to the readings received at the same base point. With the estimated error, the readings obtained at the rover can be compensated by simple subtraction. The value of the DGPS technique is a marked increase in instrument accuracy with little degradation of time requirement. The main drawback of the DGPS technique is the requirement of a second GPS receiver and corresponding

TABLE I
APPROXIMATE GPS POSITION MEASUREMENT ERROR (TOTAL) CONTRIBUTING FACTORS AND ESTIMATES

Error contributing factor	Approximate error (m)	
	Standard GPS	DGPS
Selective availability (SA)	30.0	0.0
Ionospheric variation	5.0	0.4
Inaccurate orbital path	2.5	0.0
Satellite clock	1.5	0
Multipath signal error	0.6	0.6
Tropospheric variation	0.5	0.2
Receiver noise	0.3	0.3

TABLE II
TYPICAL POSITION ACCURACY OF GPS IN (m)

	Standard GPS	Differential GPS
Horizontal	50	1.3
Vertical	78	2.0
Three dimensional	93	2.8

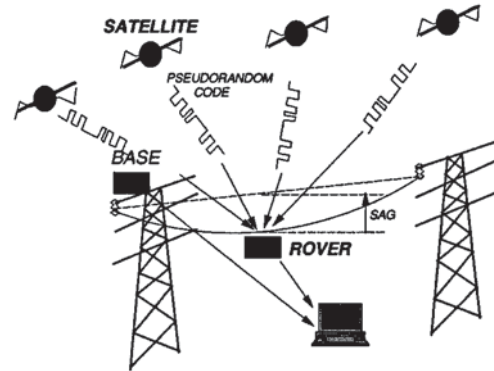


Fig. 1. Basic DGPS configuration for conductor sag measurement.

communication equipment between the base and rover instruments. Also, if the rover and base instruments are widely separated, the solution accuracy will degrade. The term direct DGPS is used to refer to a GPS configuration in which the position and time measurements are available at the rover station. The term inverse DGPS refers to a DGPS instrument in which the results are available at the base station. Table II shows typical position accuracy of GPS and DGPS [7]–[9].

III. GPS MEASUREMENT OF OVERHEAD CONDUCTOR SAG

Fig. 1 shows a proposed basic configuration of a DGPS method to measure overhead transmission conductor position and hence, sag. Inverse DGPS technology is used. Normally, only one phase of a circuit would be instrumented in a critical span.

From the base station, hard-wire is used to bring position data to power system operators. Alternately, the base station may be at the operations center itself. There is a considerable data processing burden in the implementation of the DGPS. This is needed to attenuate noise and enhance accuracy. This burden is calculable in real time using serial online processing. The main time resolution limitations of the instrument are the calculation

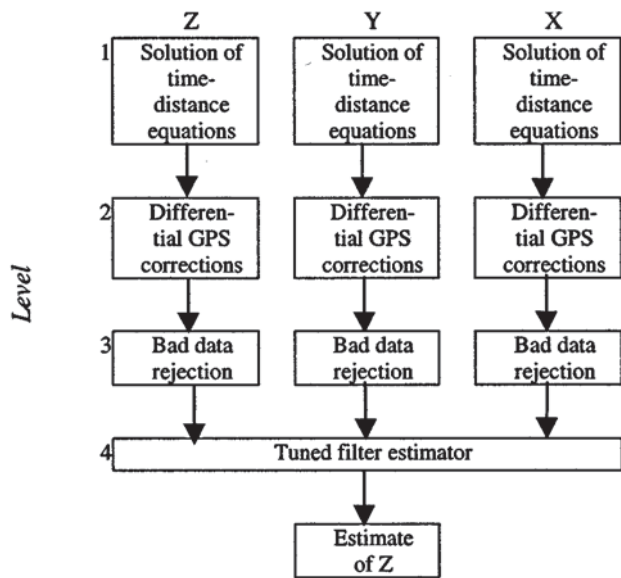


Fig. 2. Depiction of four levels of digital signal processing required for GPS measurements.

of the $(x, y, z, \text{ and } t)$ from the GPS signal and bad data rejection described in the next section.

IV. DATA PROCESSING FROM THE GPS

The accuracy of GPS measurements depends heavily on the configuration of the receiver(s) (e.g., standard GPS or differential), parameters that influence error in measurements, the number and position of the satellites in view, and the digital signal processing of the GPS measurements. The fundamental required data processing is the solution of the time-distance linear equations

$$\text{distance} = (\text{velocity})(\text{time})$$

for the four or more GPS measurements. The form of these equations is shown in (1). These equations are usually solved recursively using a previously solved case as an initialization.

This is shown in Fig. 2 as the first level of required digital processing. In the case of the application of DGPS measurements, the application of the correction signal from a base station receiver is also fundamental. This is shown in Fig. 2 as a second level signal processing. The first and second levels of processing are done entirely by the GPS engine. The central focus of interest in the measurement of overhead transmission conductor sag is in the measurement of altitude, that is $z(t)$.

In level 3 of the data processing, bad data rejection is used. Bad data result from a variety of causes, some not fully understood. The momentary loss of some satellites from view will negatively impact the measurement accuracy. Also, momentary interference and signal reflections may degrade accuracy. In addition, the ambient noise impacts solution accuracy. Other error mechanisms may also create single datum values that are erroneous.

Identification of bad data is accomplished through the use of the identification of a measurement that differs from the mean

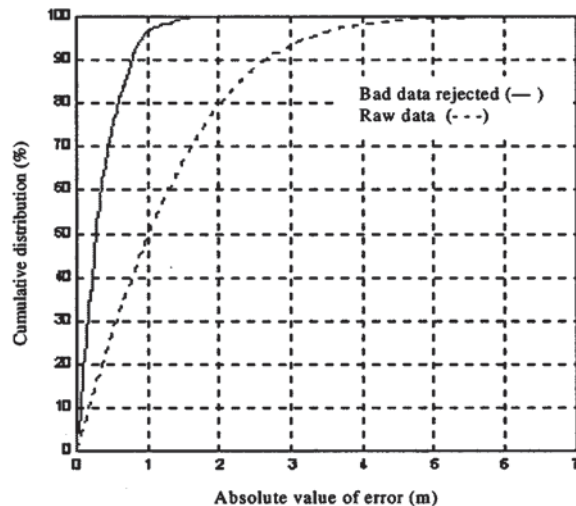


Fig. 3. Effect of bad data rejection.

value (of $x, y, \text{ or } z$ as appropriate) by greater than preset tolerance values $k\sigma_x, k\sigma_y, k\sigma_z$ respectively, where the σ values denote the sample standard deviation values of $x, y, \text{ and } z$, as measured in a moving window of width T . The bad datum is replaced with the window mean. Parameter k is chosen to obtain the proper rejection rate, and the window width T is chosen shorter than the expected duration of residence of the conductor in a given position. Typical values for the present application are $k = \pm 1.0$ and $T = 30$ s. Considerations in the selection of these parameters are: expected wind conditions and movement of the conductor, operators' requirements of real time values, and accuracy of the readings. It should be pointed out that choosing a large T implies the introduction of certain delay, since the readings of the previous positions may be still in the window. On the other hand, a very short window width will produce no rejection.

The effect of the bad data rejection can be observed in Fig. 3, which shows the cumulative distribution of the absolute value of the error computed from measurements taken for a set of known positions. The results depicted in Fig. 3 were obtained experimentally using a 12 channel DGPS receiver at a surveyed position near Phoenix, AZ, at about 359 m above mean sea level taking readings at the rate of one per second.

A fourth level of digital signal processing is depicted in Fig. 2. Note that the measurements are made at approximately 0.9 s intervals, and the measured data is available at discrete values of time. For this reason, it is convenient to refer to the measured set of data as $x(k), y(k), z(k)$. The time measurement is not used in this application. Field trials of a prototype instrument indicate that errors in x and y often occur simultaneously with errors in z . This suggests that measured x and y could provide additional information for corrections in z . In this fourth level of signal processing, two different techniques have been tested: a least squares estimator (LSE) and an artificial neural network estimator (ANNE). Both are separately used as tuned filter estimators that are trained (tuned) using a known data set. Surveyed data are used to provide a set of $[x_k, y_k, z_k]$ data, which are used to select parameters of the estimators such that the error in the known set is minimized. For testing purposes, the data

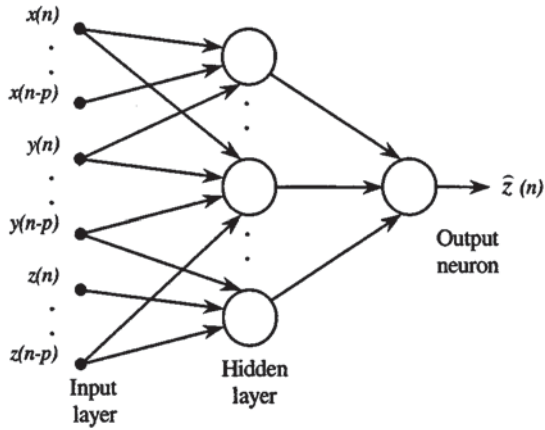


Fig. 4. ANN parameter estimator for correcting $z(n)$ data from DGPS measurement.

set allows the comparison of estimated x , y , z to known values thereby providing an estimate of the instrument accuracy.

In trying to capture the nonlinear behavior of the error, the LSE adopted is formulated as

$$\hat{z}(n) = Ax(n) + By(n) + Cz(n) + Dx^2(n) + Ey^2(n) + Fz^2(n)$$

where $x(n)$, $y(n)$, and $z(n)$ are the sampled readings at certain time that produce the corresponding vertical measurement estimation $\hat{z}(n)$. Using the set of measurements $x(n)$, $y(n)$, $z(n)$ taken for a set of known altitude z_o and replacing $\hat{z}(n)$ with z_o , the previous equation can be expressed in matrix form as

$$Z_{Known} = X\Theta$$

where $\Theta = [A \ B \ C \ D \ E \ F]^T$. The parameters $[A, B, C, D, E, F]$ are computed using simple state estimation (i.e., least squares parameter estimation). One formulation involves the Moore–Penrose pseudo-inverse of the matrix X [10]. The ANNE is implemented using a time lag feed forward network [11]. In this configuration, contrary to the LSE, p previous readings of x , y and z are used to estimate z . A two-weighted layer network is used, consisting of h neurons in the hidden layer and one output layer. A sigmoid function, specifically the logistic function [11] is employed as the activation function of the hidden neurons, while the output neuron employs a linear function. The optimum values of p and h are determined in the tuning process. A schematic of the network is shown in Fig. 4.

Some results of field testing and the details of the signal processing techniques described here are shown in the Appendix. Note that through the use of a least squares estimator, accuracy within 21.5 cm was obtained 70% of the time, and using an ANNE, an accuracy of at least 19.6 cm is obtained for 70% of the time (see Table IV).

V. POWER SUPPLY AND COMMUNICATIONS LINK

For a practical sag measurement instrument, in addition to the digital signal processing outlined previously, there is the matter of instrument power supply and the communication link

TABLE III
INSTRUMENT POWER REQUIREMENTS (TYPICAL)

Unit	Component	Typical power requirements (DC)		
		V (volts)	I (amps)	P (watts)
Rover	GPS receiver	12	2	24
	Digital (serial) data transmitter	12	2	24
	Digital (serial) data receiver	12	0.2	2.4
Base	GPS receiver	12	2	24
	Digital (serial) data transmitter	12	5	60
	Digital (serial) data receiver	12	0.2	2.4

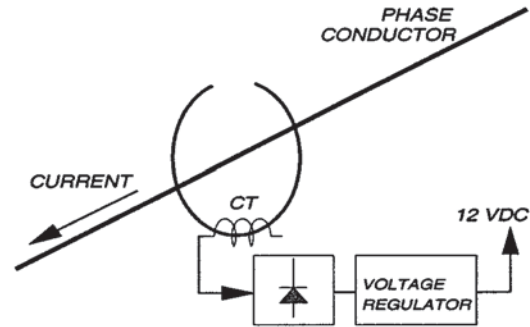


Fig. 5. Power supply for the rover unit: a magnetic ring is clamped around the conductor to be instrumented.

between the base and rover units. Based on a popular commercial GPS receiver, the power supply requirements for the base and rover instruments are shown in Table III. The power requirements at the base station are derived from conventional sources. At the rover, power must be derived from the overhead conductor itself. This concept has been commercialized in many applications, and laboratory tests revealed that the technology is easily implemented. Fig. 5 shows one configuration based on a current transformer (CT) design. Experience shows that voltage regulation of the GPS receiver supplies is essential.

Communication between the rover and base station is accomplished using standard digital communications technologies. A typical communication link consists of “on–off” amplitude modulation for the communication channel, implemented in the Industrial Scientific and Medical (ISM) band, 902–928 MHz. The design tested in the laboratory is effectively a serial port connection via radio. Fig. 6 shows a possible configuration. The frequency source in this design is derived from a voltage-controlled oscillator (VCO) which is held at the proper frequency by a phase locked loop circuit. The ultimate frequency source is a quartz crystal (XTAL).

An important issue in the present application is the performance of the communication link in a high voltage environment (and, perhaps more serious, the 1.5-GHz band reception of the GPS signal at the rover). Experiments have been done to determine the difficulties in these areas and the main conclusion is

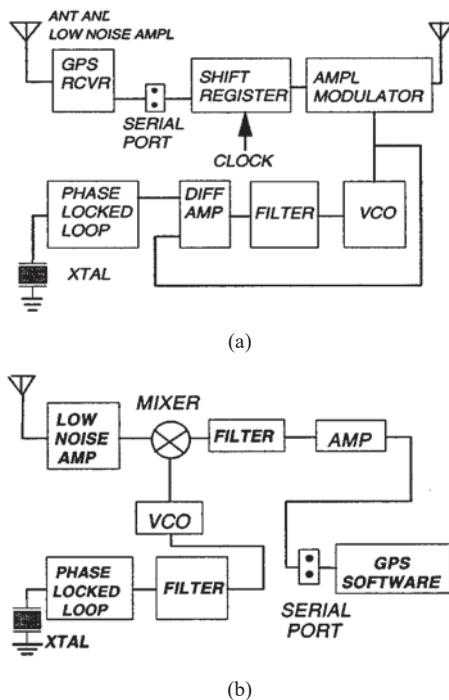


Fig. 6. Communication between the rover and base stations.

that corona creates potentially intolerable conditions for radio reception in the 930-MHz and 1.5-GHz bands. There may also be some degree of “saturation” in the receiver front-end first stages, but the use of low noise amplifiers, standard in ISM and GPS technologies, seems to be adequate. It is important that the radio receivers at the rover be far from any corona. The receiver should be “shielded” by instrument packaging that is smooth and corona free.

VI. CONCLUSION

The main conclusion of this study is that DGPS technology is feasible for the direct instrumentation of overhead power line conductor sag measurement. The accuracy of such an instrument is in the range of 19.6 cm 70% of the time. The method utilizes two GPS receivers, one as a base station that must be at an accurately surveyed location. The instrument can be designed such that the rover receiver operating power is taken from the line. Care must be taken in the design of the instrument package because of the potential of interference from corona. The main digital signal processing needed to obtain accurate z measurements are bad data rejection, least squares parameter estimation, or artificial neural network filtering.

Although the subject of dynamic line ratings is not considered in this paper, it is believed that real time sag measurement can be translated into real time dynamic circuit ratings, and this is expected to have value in the sale of transmission capacity.

APPENDIX

A. Signal Processing Results

In order to test the previously described signal processing procedures, a series of tests were done. One exemplar test is described as taking DGPS readings for ten known elevations

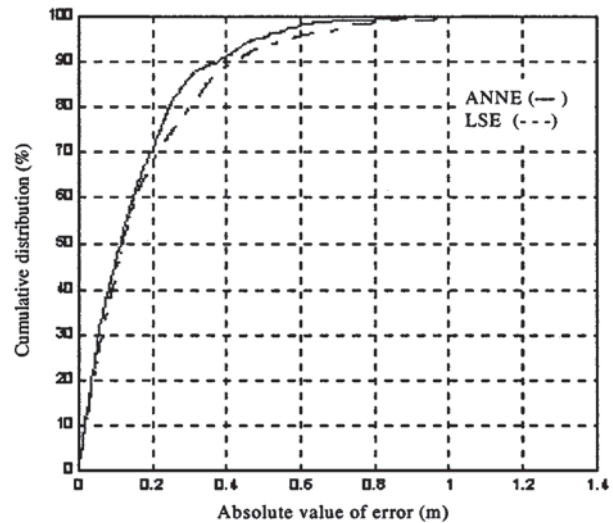


Fig. 7. Cumulative error for LSE and ANNE.

TABLE IV
ACCURACY ACHIEVED BY LSE AND ANNE

Confidence Index (%)	Absolute error (cm)			
	Raw data	Bad data rejected	LSE	ANNE
90	264.4	78.5	41.9	37.4
80	201.8	58.9	30.1	24.5
70	161.1	45.5	21.5	19.6
60	128.9	34.9	15.4	14.6
50	100.6	27.9	11.8	11.4

(stations), collocated in longitude and latitude. The altitude difference between stations varies between 0.10 to 1.0 m. An average of 1800 readings were taken for each station. From the ten stations, five were used to tune the estimators and the rest were used to test the performance of the estimators in the presence of data not previously seen. The bad data rejection in the third level has been computed using values of $k = 1$ and $T = 30$ s. These have presented a good performance regarding excessive number of data rejection and the response time, as explained previously. For the ANNE, several configurations have been explored regarding the number of neurons in the hidden layer. Good results were obtained for $h = 4$. In all cases, the number of previous readings used have been $p = 9$. With the configurations described the results obtained are summarized in Fig. 7.

It can be seen that for a 90% confidence the LSE and ANNE present, respectively, an accuracy of 41.9 cm and 37.4 cm. For 70% confidence, the respective accuracies are 21.5 cm and 19.6 cm. Table IV summarizes the accuracy obtained with the respective confidence index. In Fig. 7 and Table IV, note that there are some additional 5 cm uncertainty in the antenna position, and at least 5 cm potential survey error. It is expected that the inaccuracies tabulated are conservative. It can be seen that the ANNE presents slightly better results. However, both estimators present similar performance.

ACKNOWLEDGMENT

The authors would like to thank their colleagues at Entergy and the Arizona Public Service Company. They would also like to thank Prof. E. Burns, Prof. R. Farmer, and Prof. G. Karady, Arizona State University (ASU), Tempe, D. Selin, APS, A. Hunt, ASU, for designing the initial DGPS receiver circuit, and several students who assisted in the power supply and communications link designs. They would also like to thank J. Wells, United States Navy, for power supply design, and R. Faulkner and A. Carbognin for the loan of GPS receivers from NovAtel Inc., Calgary, BC, Canada. This work was performed at the ASU Center for the Advanced Control of Energy and Power Systems, Tempe.

REFERENCES

- [1] G. Ramon, IEEE Task Force Chairman, "Dynamic thermal line rating summary and status of the state-of-the-art technology," *IEEE Trans. Power Delivery*, vol. PWRD-2, pp. 851–856, July 1987.
- [2] *IEEE Standard for Calculating the Current-Temperature Relationship of Bare Overhead Conductors*, 1993.
- [3] T. Seppa, "Accurate ampacity determination: Temperature-sag model for operational real time ratings," *IEEE Trans. Power Delivery*, vol. 10, pp. 1460–1466, July 1995.
- [4] U. Fernández, C. Mensah-Bonsu, J. Wells, and G. Heydt, "Calculation of the maximum steady state transmission capacity of a system," in *Proc. 30th North American Power Symp.*, Cleveland, OH, Oct. 19–20, 1998, pp. 300–305.
- [5] D. Douglas and A. Edris, "Real-time monitoring and dynamic thermal rating of power transmission circuits," *IEEE Trans. Power Delivery*, vol. 11, pp. 1407–1415, July 1996.
- [6] B. J. Cory and P. F. Gale, "Satellites for power system applications," *IEEE Power Eng. J.*, vol. 7, Oct. 1993.
- [7] J. Hurn, *Differential GPS Explained*. Sunnyvale, CA: Trimble Navigation Ltd., 1993.
- [8] E. Kaplan, "Understanding GPS: Principles and applications," 1996.
- [9] T. Gray, *NAVSTAR GPS and DGPS*: CSI, 1997.
- [10] G. Heydt, *Computer Analysis Methods for Power Systems*. Scottsdale, AZ: Stars in a Circle, 1998.
- [11] S. Haykin, *Neural Networks: A Comprehensive Foundation*, 2nd ed. New York: Prentice-Hall, 1999.
- [12] D. G. Fink and H. W. Beaty, Eds., *Standard Handbook for Electrical Engineers*. New York: McGraw-Hill, 1993.

Chris Mensah-Bonsu (M'00) was born in Kumasi, Ashanti, Ghana. He received the M.A. degrees in control systems and electric power engineering from Cleveland State University, Cleveland, OH, and the Higher Institute of Mechanical and Electrical Engineering, Varna, Bulgaria, respectively. He is currently pursuing the Ph.D. degree at Arizona State University, Tempe.

Ubaldo Fernández Krekeler (S'01) was born in Asunción, Paraguay. He received the degree in ingeniería electromecánica from the Universidad Nacional de Asunción, and the M.S.E.E. degree from Arizona State University, Tempe, in 1999.

Mr. Krekeler is a winner of a Fulbright Fellowship award.

Gerald Thomas Heydt (M'71–SM'79–F'91) received the Ph.D. degree from Purdue University, West Lafayette, IN.

He is the author of two books in Electric Power Engineering. Dr. Heydt is presently a Professor of Electrical Engineering and Center Director at ASU.

Dr. Heydt is a member of the National Academy of Engineering and recipient of the 1995 Power Engineering Society's "Power Engineering Educator of the Year" award.

Yuri Hoverson was born in Scottsdale, AZ, and is pursuing the B.S.M.E. degree at Arizona State University, Tempe.

He was with the U. S. Navy.

Mr. Hoverson is the 1999 recipient of the Salt River Project Energy and Environment Scholarship.

John Schilleci (M'71–SM'87) was born in New Orleans, LA. He received the B.S.E.E. degree from Louisiana State University, Baton Rouge.

He has been in the electric utility business for the last 32 years with experience in substation, transmission, distribution, metering, and communications. He is an Adjunct Faculty Member of the Electrical Engineering Department, University of New Orleans.

Baj L. Agrawal (M'74–SM'83–F'94) was born in Kalaiya, Nepal. He received the B.S. degree in electrical engineering from Birla Institute of Technology and Science, Birla, India, and the M.A. and Ph.D. degrees in control systems from the University of Arizona, Tempe.

He joined the Arizona Public Service Company in 1974, where he is currently a Senior Consulting Engineer. He is a registered professional engineer in the state of Arizona and is a Member of the IEEE SSR Working Group.